Journal of the Optical Society of America A
OPTICS, IMAGE SCIENCE, AND VISION

Low-reflection region within the stop band of a finite or absorbing periodic multilayer

JOHN LEKNER

School of Chemical and Physical Sciences, Victoria University of Wellington, P.O. Box 600, Wellington, New Zealand (john.lekner@vuw.ac.nz)

Received 24 March 2016; revised 5 July 2016; accepted 11 July 2016; posted 12 July 2016 (Doc. ID 261605); published 2 August 2016

Nonabsorbing periodic multilayers reflect both the *s*(TE) and *p*(TM) polarizations strongly within the respective stop bands. We find that finite or weakly absorbing layers, for which the reflection is usually strong within the stop bands, can have zero or very weak reflection of the *p* polarization near the middle of the stop band, close to glancing incidence. Approximate expressions are derived for the location (in angle of incidence and frequency) of the reflection minimum and compared with calculated reflectances for specific multilayers.

OCIS codes: (160.5293) Photonic bandgap materials; (240.6690) Surface waves; (240.6680) Surface plasmons; (350.4238) Nanophotonics and photonic crystals.

http://dx.doi.org/10.1364/JOSAA.33.001648

1. INTRODUCTION

We have found a deep minimum in the reflectance of the *p* polarization from *absorbing* periodically stratified media, remarkable in that it is localized within the stop band of the nonabsorbing stratification. This phenomenon does not seem to have been noticed by workers in the field [1–5].

Finite *nonabsorbing* periodically stratified media show the same effect: in fact, *zero* reflection of the *p* polarization is possible within the stop band (the stop band is of course that of an infinite structure; within the stop band, waves are exponentially damped and reflection is total).

There is no anomaly in the *s* reflectance, which is strong within the entire *s* stop band, as expected.

This paper aims to quantify the location and depth of the *p* reflectance minimum, which we interpret as *due to destructive interference of the multiple reflected waves* at a precise frequency and angle of incidence.

We begin in Section 2 with a summary of the results for reflection of the *p* polarization by a finite periodic stack, such as that shown in Fig. 1 for $N = 4$ periods of a high–low structure. Section 3 then gives the reflectivity curves for $N = 1, 2,$ and 3, with analytical results for the location of the zero of R_p for $N = 1$, and numerical results for $N = 2$ and 3. Sections 4 and 5 consider reflection of the *p* polarization by *absorbing* periodic media.

All of the figures and numeric results in this paper are for $ZnS|MgF_2$ high–low multilayers which are quarter-wave stacks at normal incidence. Similar results were obtained for the $HfO_2|SiO_2$ multilayers of Ref. [2].

Figure 1 shows the dielectric profile of a four-period $\lambda/4$ stack, which by design reflects strongly at normal incidence within the "stop band," namely, within the angular frequency range $\omega_0 - \Delta\omega < \omega < \omega_0 + \Delta\omega$, where (see, for example, Section 12.3 of [6])

$$\frac{\Delta\omega}{\omega_0} = \frac{2}{\pi} \arcsin \frac{n_h - n_\ell}{n_h + n_\ell}. \tag{1}$$

The thicknesses of the high- and low-index materials are chosen to be $h = \lambda/4n_h$, $\ell = \lambda/4n_\ell$, where n_h, n_ℓ are the refractive indices, λ is the vacuum wavelength, and the central angular frequency is given by

$$\omega_0 = (\pi/2)(c/n_h h) = (\pi/2)(c/n_\ell \ell). \tag{2}$$

2. REFLECTION BY A FINITE PERIODIC STRUCTURE

The *p* reflection amplitude r_p, from which we find the reflectance $R_p = |r_p|^2$, is given by {[6], Eqs. (13.44) and (13.49)}

$$-r_p = \frac{Q_1 Q_2 m_{12} + m_{21} + iQ_1(m_{22} - \sigma_N) - iQ_2(m_{11} - \sigma_N)}{Q_1 Q_2 m_{12} - m_{21} + iQ_1(m_{22} - \sigma_N) + iQ_2(m_{11} - \sigma_N)}, \tag{3}$$

$$\sigma_N = \cos\phi - \sin\phi \cot(N\phi),$$
$$\cos\phi = \frac{1}{2} \operatorname{trace} M = \frac{1}{2}(m_{11} + m_{22}), \tag{4}$$

$$Q_1 = \frac{q_1}{\epsilon_1}, \qquad Q_2 = \frac{q_2}{\epsilon_2},$$
$$q_1 = \frac{\omega}{c}(\epsilon_1 - \epsilon_1 \sin^2\theta)^{\frac{1}{2}} = \frac{\omega}{c} n_1 \cos\theta,$$
$$q_2 = \frac{\omega}{c}(\epsilon_2 - \epsilon_1 \sin^2\theta)^{\frac{1}{2}}. \tag{5}$$

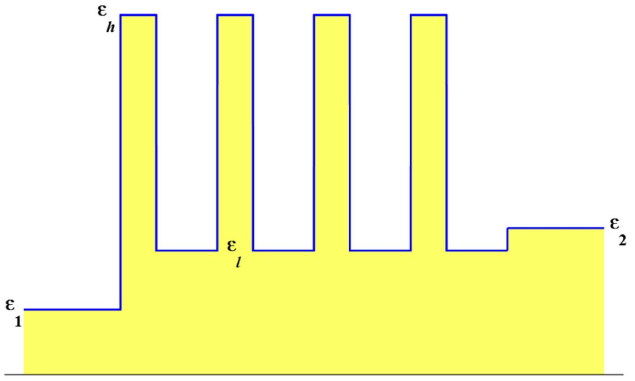

Fig. 1. $(HL)^4$ high–low dielectric mirror, drawn for $n_1 = 1$(air), $n_2 = 1.5$(glass), $n_h = 2.35$(ZnS), $n_\ell = 1.38(MgF_2)$. The dielectric constant values are the squares of the refractive indices, $\epsilon = n^2$. The figure is drawn to scale for a $\lambda/4$ stack, for which the thicknesses of the high and low dielectric layers are as given in the text.

In Eqs. (3) and (4), m_{ij} are the elements of M, the 2×2 matrix of a single period. The matrix is unimodular: $\det M = m_{11}m_{22} - m_{12}m_{21} = 1$. For nonabsorbing media the matrix elements are real, and thus so is $\cos\phi$, even within the stop band of an infinite stack, where $\cos^2\phi > 1$, and ϕ itself is complex. When $\cos\phi$ is real, so are the σ_N, which are rational functions of $\cos\phi$. For example,

$$\sigma_1 = 0, \qquad \sigma_2 = \frac{1}{2\cos\phi}, \qquad \sigma_3 = \frac{2\cos\phi}{(2\cos\phi)^2 - 1},$$
$$\sigma_4 = \frac{(2\cos\phi)^2 - 1}{2\cos\phi[(2\cos\phi)^2 - 2]}. \tag{6}$$

Thus the σ_N are rational functions of trace $M = m_{11} + m_{22}$.

For the high–low dielectric mirror of Fig. 1, the matrix M may be written down explicitly in terms of the normal components q_h, q_ℓ of the wave-vectors within the high- and low-index materials,

$$q_h = \frac{\omega}{c}(\epsilon_h - \epsilon_1 \sin^2\theta)^{\frac{1}{2}} \qquad q_\ell = \frac{\omega}{c}(\epsilon_\ell - \epsilon_1 \sin^2\theta)^{\frac{1}{2}}, \tag{7}$$

where ϵ_h and ϵ_l are the dielectric constants of the high- and low-index materials, equal to the squares of the refractive indices. We define

$$c_h = \cos q_h h, \qquad c_\ell = \cos q_\ell \ell, \qquad s_h = \sin q_h h,$$
$$s_\ell = \sin q_\ell \ell, \tag{8}$$

$$Q_h = q_h/\epsilon_h, \qquad Q_\ell = q_\ell/\epsilon_\ell. \tag{9}$$

Then the p polarization unit cell matrix becomes [6,7]

$$M = \begin{pmatrix} c_\ell c_h - (Q_h/Q_\ell)s_\ell s_h & c_\ell s_h/Q_h + c_h s_\ell/Q_\ell \\ -Q_\ell s_\ell c_h - Q_h s_h c_\ell & c_\ell c_h - (Q_\ell/Q_h)s_\ell s_h \end{pmatrix}. \tag{10}$$

It follows from Eqs. (4) and (10) that, for this simple high–low periodic structure, the phase parameter ϕ is given by

$$\cos\phi = c_\ell c_h - \frac{1}{2}\left(\frac{Q_h}{Q_\ell} + \frac{Q_\ell}{Q_h}\right)s_\ell s_h. \tag{11}$$

3. ZERO R_p FOR A FINITE PERIODIC STACK

For *one* period, namely, just one high-index layer followed by a low-index layer, the p reflection amplitude is, from Eqs. (3) and (6),

$$-r_p = \frac{Q_1Q_2m_{12} + m_{21} + iQ_1m_{22} - iQ_2m_{11}}{Q_1Q_2m_{12} - m_{21} + iQ_1m_{22} + iQ_2m_{11}} \qquad (N = 1). \tag{12}$$

If both the high- and low-index materials have negligible absorption, all the matrix elements are real and there will be zero reflection of the p wave if

$$Q_1Q_2m_{12} + m_{21} = 0 \quad \text{and} \quad Q_1m_{22} - Q_2m_{11} = 0. \tag{13}$$

On inserting the matrix elements from Eq. (10), these equations reduce to

$$Q_H \tan q_h h + Q_L \tan q_l l = 0 \quad \text{and}$$
$$P - \tan q_h h \tan q_l l = 0, \tag{14}$$

where

$$Q_H = \frac{Q_1Q_2}{Q_h} - Q_h, \qquad Q_L = \frac{Q_1Q_2}{Q_l} - Q_l,$$
$$P = \frac{Q_1 - Q_2}{\frac{Q_1Q_l}{Q_h} - \frac{Q_2Q_h}{Q_l}}. \tag{15}$$

These equations are satisfied by

$$\tan^2 q_h h = -\frac{PQ_L}{Q_H}, \qquad \tan^2 q_l l = -\frac{PQ_H}{Q_L}. \tag{16}$$

We note that the right-hand sides of Eq. (16) are independent of frequency, and so is the ratio

$$\frac{q_h h}{q_l l} = \frac{\arctan\sqrt{-\frac{PQ_L}{Q_H}}}{\arctan\sqrt{-\frac{PQ_H}{Q_L}}}. \tag{17}$$

This equation may thus be solved for the angle of incidence θ, and this angle can be substituted into either of the equations in Eq. (16) to find the frequency. (A physical solution exists only if the signs of Q_H, Q_L, and P are such as to give real tangents, of course.) For the one-period stack, and the parameters of Fig. 1, the solutions are $\theta \approx 73.4°$, $\omega \approx 1.083\omega_0$. This point of zero reflection is shown in Fig. 2 as a diamond. A wide minimum surrounds this zero of reflectivity, but the region of small reflection gets more localized as the number of layers N increases, as we shall see.

The p stop band of the *infinite* stack, calculated using Eqs. (13.71) and (13.72) of [6], is bounded in Figs. 2–5 by the thick curves of light shading. These correspond to $\cos^2\phi = 1$.

We see from the figures that for $N = 2$ and $N = 3$, the zero of R_p moves closer to glancing incidence: $(N, \theta, \omega/\omega_0)$ values at $R_p = 0$ are (2, 80.1°, 1.19), (3, 83.7°, 1.21). (These were found numerically.) Continuing to increase N, we find that the minimum gets narrower in both angle and frequency, and closer to glancing incidence. For nonabsorbing media, the interference minimum disappears, defeated by the twin powers of the stop band and the necessity of full reflection at glancing incidence.

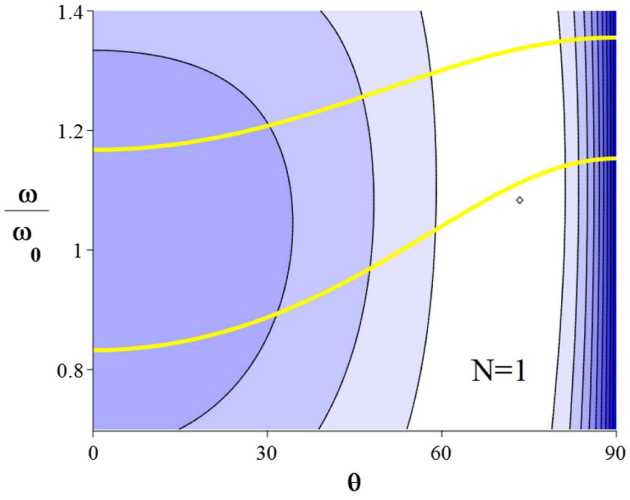

Fig. 2. Reflectance R_p of a single period HL of the quarter-wave stack of Fig. 1. The figure shows the contours of R_p as a function of the angle of incidence and of the frequency. Dark shading corresponds to strong reflectivity. The reflectance contours, here and in the figures that follow, are at $R_p = 0.1(0.1)0.9$, with $R_p < 0.1$ white and $R_p > 0.9$ the darkest.

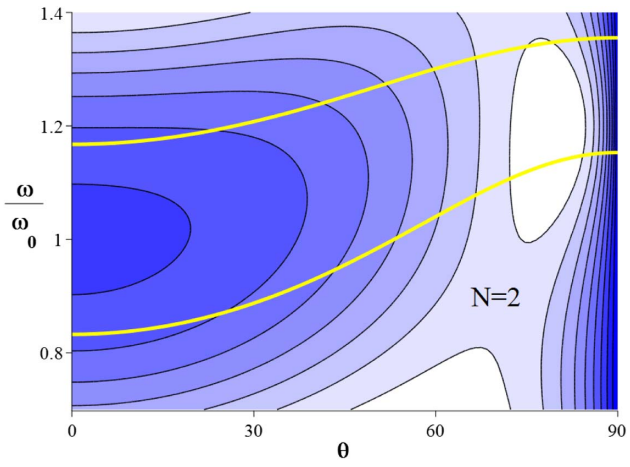

Fig. 3. R_p for two periods $(HL)^2$ of the quarter-wave stack of Fig. 1. The figure contours and shading are as in Fig. 2. Note the minimum developing within the stop band, the lower and upper limits of which are indicated by the light curves.

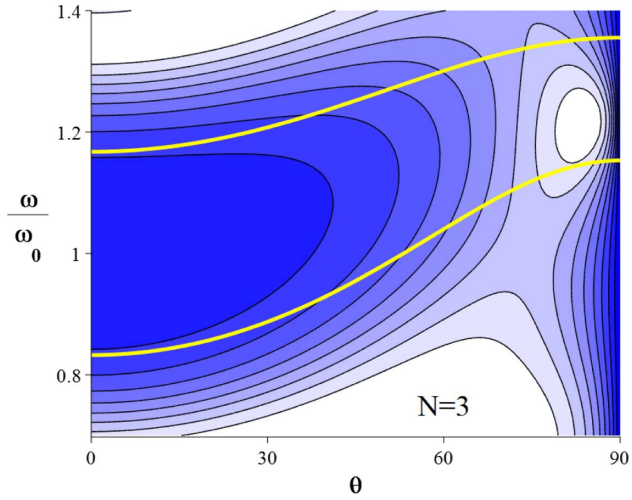

Fig. 4. R_p for three periods $(HL)^3$ of the quarter-wave stack (indices as in Fig. 1). The reflectivity contours and shading are as in Fig. 2. Note the stronger reflection within the stop band and the more localized reflection minimum. The reflectance tends to unity at glancing incidence, in accordance with a general theorem ([6], Section 2.3).

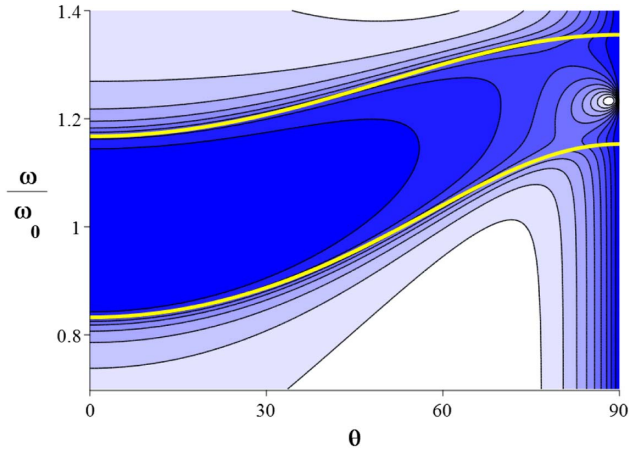

Fig. 5. Reflectance R_p of an *absorbing* quarter-wave stack of Fig. 1. The number of periods N is assumed to be large enough so that R_p can be calculated as the absolute square of either of the expressions in Eq. (19), which require $N|\mathrm{Im}(\phi)| \gg 1$. The absorption in both high- and low-index materials is modeled by complex refractive indices: $n_h = 2.35 + 0.01i$, $n_\ell = 1.38 + 0.01i$.

4. REFLECTION BY AN ABSORBING PERIODIC MEDIUM

A recent paper has explored reflection by absorbing periodically stratified media [7]. The main effects of absorption are the smoothing and rounding of the reflectance curves and the existence of limiting forms of the s and p reflection amplitudes, which are independent of the substrate properties and of the number N of the stratification periods. Both of these effects may be expected on physical grounds, since absorption decreases the long-range interference and limits wave penetration to the substrate.

Absorption can be represented by (usually small) imaginary parts of the refractive indices, and thus of the dielectric functions:

$$n \to n + ik, \qquad \epsilon \to n^2 + 2\,\mathrm{i}\,n\,k - k^2. \tag{18}$$

As explained in Section 13.2 of [6], for nonabsorbing media, stop bands (and strong reflection) correspond to $\cos^2\phi > 1$ and complex ϕ. When there is absorption, represented by complex dielectric functions and refractive indices, the corresponding normal components of the wave-vectors also become complex, as do the matrix elements. Then ϕ is always complex,

but for weak absorption the stop-band structure usually dominates.

The p reflection amplitude r_p, from which we find the reflectance $R_p = |r_p|^2$, is given by {[7], Eq. (23)}

$$-r_p = \frac{Q_1 M_{12} - i(M_{11} - \sigma)}{Q_1 M_{12} + i(M_{11} - \sigma)} = \frac{M_{21} + iQ_1(M_{22} - \sigma)}{-M_{21} + iQ_1(M_{22} - \sigma)}. \tag{19}$$

Here, M_{ij} are the (now complex) elements of the 2×2 matrix of one period of the stratification and $Q_1 = q_1/n_1^2 = (\omega/c)n_1^{-1} \cos\theta$, where n_1 and q_1 are the refractive index and normal component of the wave-vector in the medium of incidence (assumed nonabsorbing). The quantity σ, which is the absorbing large N limit of σ_N, is shown in [7] to take one of two possible values (depending on which has the smaller modulus):

$$\sigma_\pm = \exp(\pm i\phi) = \cos\phi \pm i \sin\phi,$$
$$\phi = \arccos \frac{1}{2}(M_{11} + M_{22}). \tag{20}$$

We note that the expressions in Eq. (19) are equivalent because the one-period matrix is unimodular,

$$M_{11}M_{22} - M_{12}M_{21} = 1, \tag{21}$$

and because σ satisfies the quadratic equation {[7], Eq. (14)}

$$\sigma^2 - (M_{11} + M_{22})\sigma + 1 = 0. \tag{22}$$

Note also that the refractive index n_2 of the substrate and the number N of the stratification periods do not appear in the reflection amplitude expressions (19). These expressions apply when the product of N and the imaginary part of ϕ is large compared to unity. (Near the reflectivity minimum in Fig. 5, $\mathrm{Im}\,\phi$ has magnitude of ~0.25. Most of $\mathrm{Im}\,\phi$ is due to the position inside the stop band; only about 1% comes from the absorption.)

The results listed so far are for any periodic stratification, that is, for any periodic variation of the dielectric function $\epsilon(z) = n^2(z)$. The most tractable, theoretically and experimentally, is the periodic structure of alternating high and low indices, as shown in Fig. 1. For this special case, the matrix M was written down explicitly in Eq. (10) in terms of the normal components q_h, q_ℓ of the wave-vectors within the high- and low-index materials [$\epsilon_h = (n_h + ik_h)^2$, $\epsilon_\ell = (n_\ell + ik_\ell)^2$].

The normal incidence reflectivity of an absorbing quarter-wave stack, such as drawn in Fig. 1 but with small imaginary parts of the refractive indices, was shown in Fig. 1 of [7] and shows the expected rounding of the reflectivity from total reflection within the stop band. At normal incidence, there is no difference between the s and p reflectivities.

In Figs. 5 and 6, we plot the p reflectivity contours for an absorbing quarter-wave stack. As in the finite nonabsorbing case, there is strong reflection within the stop band except for the deep minimum inside the stop band: $R_p \approx 0.016$ at $\theta \approx 88.5°$, $\omega/\omega_0 \approx 1.23$ for the parameters chosen. The location and width of the minimum depends on the degree of absorption in both the high-index and low-index materials. For example, as the imaginary parts of the refractive indices decrease toward zero, the minimum in Fig. 5 disappears. If, instead of the parameters of Figs. 5 and 6, we put $n_h = 2.35 + 0.02i$, $n_\ell = 1.38$, the minimum is weaker than if we put $n_h = 2.35$, $n_\ell = 1.38 + 0.02i$. For large absorption, the reflectance contours resemble those of a stack with small N.

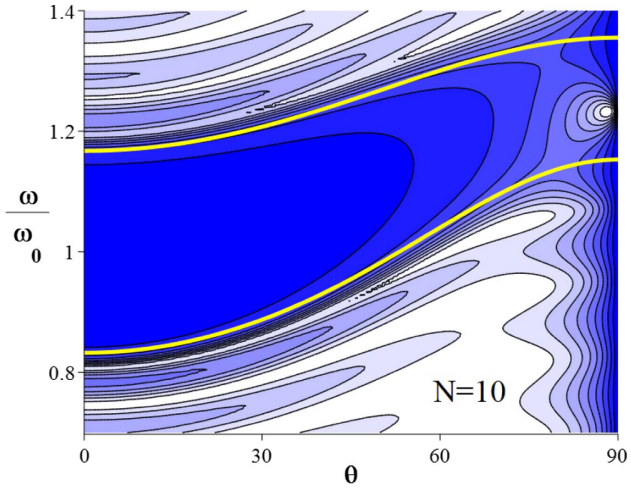

Fig. 6. Reflectance R_p of an absorbing quarter-wave stack, with the same parameters as in Fig. 5, calculated for $N = 10$. Note that the reflectance is similar to that of Fig. 5 inside the stop band, but shows oscillations outside the stop band.

$N\,\mathrm{Im}(\phi)$ is largest inside the stop band, and therefore so is the agreement between Figs. 5 and 6. As N increases from its value 10 in Fig. 6, the reflectance within the stop band approaches that in Fig. 5 but more oscillations appear outside the stop band. These oscillations have been smoothed by the theory (which assumes $N\,\mathrm{Im}(\phi)$ to be large everywhere) in Fig. 5.

5. LOCATION OF THE R_p MINIMUM

From Eqs. (20) or (22), we see that the parameters $\sigma_\pm$ which enter the reflection amplitude expressions in Eq. (19) can be written as

$$\sigma_\pm = \frac{1}{2}(M_{11} + M_{22}) \pm \frac{1}{2}([M_{11} + M_{22}]^2 - 4)^{\frac{1}{2}}. \tag{23}$$

Hence the combination $M_{11} - \sigma$, which enters into the first p reflection amplitude in Eq. (19), is given by

$$M_{11} - \sigma_\pm = \frac{1}{2}(M_{11} - M_{22}) \mp \frac{1}{2}([M_{11} + M_{22}]^2 - 4)^{\frac{1}{2}}. \tag{24}$$

The two terms on the right of Eq. (24) have equal magnitude when $M_{11}M_{22} = 1$. For absorbing media, the dielectric functions ϵ_h, ϵ_ℓ and thus also the wave-vector components q_h, q_ℓ are complex, and so are all the matrix elements. Thus, it is not possible to make $M_{11} - \sigma$ vanish but it is possible to make the real part vanish, at some frequency and angle of incidence, in which case $M_{11} - \sigma$ becomes equal to $-iS$, say. Let us also write the complex matrix elements as

$$M_{ij} = m_{ij} + ik_{ij}. \tag{25}$$

Then the reflection amplitude and reflectance (at the frequency and angle of incidence for which $M_{11} - \sigma = -iS$) are equal to

$$-r_p = \frac{Q_1(m_{12} + ik_{12}) - S}{Q_1(m_{12} + ik_{12}) + S},$$
$$R_p = \frac{(Q_1 m_{12} - S)^2 + Q_1^2 k_{12}^2}{(Q_1 m_{12} + S)^2 + Q_1^2 k_{12}^2}. \quad (26)$$

For weak absorption S is small, and so is $Q_1 = (\omega/c)n_1^{-1}\cos\theta$ near glancing incidence; hence we may be able to find an angle θ_m and frequency ω_m at which $Q_1 m_{12} = S$. Then the reflectance would become approximately

$$R_p(\theta_m, \omega_m) \approx \frac{k_{12}^2}{4m_{12}^2}. \quad (27)$$

The reflectance at minimum may thus be very small if the materials of the periodic multilayer structure are weakly absorbing ($N \gg 1$ is assumed).

To locate the reflectance minimum further, we make the simplifying assumption that it occurs close to glancing incidence, as in the example shown in Figs. 5 and 6. Near glancing incidence, $\sin^2\theta$ is nearly constant at unity, so in seeking to make the real part of $M_{11} - \sigma$ vanish, we can take $\theta \approx \frac{\pi}{2}$ and find the angular frequency ω_m at which $M_{11} - \sigma = -iS$. On the other hand, Q_1 varies rapidly near glancing incidence, going to zero as $\cos\theta$. Hence, we can substitute $\omega = \omega_m$ in the equation $Q_1 m_{12} = S$ to find θ_m.

For the $\lambda/4$ stack with the parameters of Fig. 1, we find by this procedure that the real part of $M_{11} - \sigma$ is zero at $\omega/\omega_0 \approx 1.234$ and $\omega/\omega_0 \approx 1.267$, from $m_{11}m_{22} = 1$ at glancing incidence. The larger frequency gives a negative value of S, and m_{12} of nearly zero, so it is unsuitable. The value 1.234 for the frequency ratio gives positive values of S and of m_{12}, leading to a glancing angle $90° - \theta \approx 1.456°$. Both the frequency and glancing angle are in agreement with the values 1.23,1.5° of Fig. 5. However, the expression (27), which only approximately minimizes the reflectance in Eq. (26), gives 0.020 for the reflectance at minimum compared with $R_p \approx 0.016$ found numerically.

6. SUMMARY AND CONCLUSION

We have found a minimum in the reflectance of the p polarization, localized within the stop band. This phenomenon has not been remarked on by workers in the field of reflection by *absorbing* periodically stratified media [1–5]. Of the two papers that might have seen the effect, [4] is restricted to angles of incidence less than 80° and [5] deals with periodic stacks of graphene layers, where perhaps the absorption is so strong as to drown the effect.

It is known that nonabsorbing periodic multilayers can facilitate phenomena analogous to *attenuated total reflection* ([6], Sections 10.6, 10.7, and 12.6), which is associated (for the p polarization) with electromagnetic surface waves. In attenuated total reflection, the p reflectance can have a sharp minimum in the total reflection region because of the presence of an absorbing layer, usually a conductor. The conductor normally used in attenuated total reflection can be replaced by a photonic band gap material [8], which is (as usual) entered by the light beam through a high-index material. Reference [8] gives examples of a $TiO_2|SiO_2$ multilayer which gives a low reflectance of 632.8 nm light at about 49°. Reference [9] discusses the coupling between electromagnetic surface modes and Bloch waves in multilayer stacks. Reflection minimums (at normal incidence) from a gold layer on top of a periodic GaAs|AlAs multilayer have been studied recently [10]. These correspond to the excitation of Tamm plasmons.

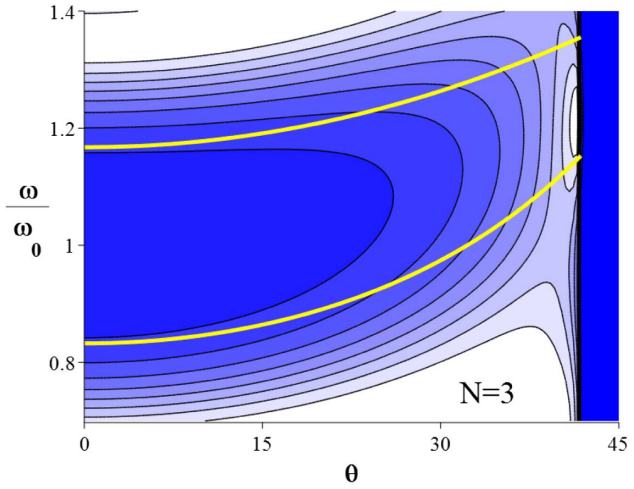

Fig. 7. Reflection by a stack of three nonabsorbing periods, with parameters as in Fig. 4 except that (with reference to Fig. 1) light enters from the right. The critical angle is $\theta_c = \arcsin 1.0/1.5 \approx 41.8°$. Note that the reflection minimum is more tightly squeezed up against the total reflection region than is the case in Fig. 4 at glancing incidence.

However, since finite nonabsorbing stacks show the reflection minimum also, the author's view is that the physical cause is simply destructive interference at very specific frequency and angle of incidence. Absorption allows the reflectivity minimum to persist in larger stacks; in effect it replaces the infinite stack with a finite one, because the attenuation allows penetration only to a finite depth.

A reviewer has suggested that it would be useful to shift the angle of incidence at which the reflectivity minimum occurs to more accessible values away from glancing incidence. This can be done by entering from a medium of higher index than that of the substrate and using a low–high multilayer instead of the high–low configuration. Total reflection for $\theta \geq \theta_c = \arcsin n_2/n_1$ then locates the minimums at just below the critical angle θ_c. Figure 7 gives an example.

Acknowledgment. The author thanks Eric Le Ru for stimulating discussions, and in particular for suggesting that finite stacks might show the same phenomenon. The reviewers' comments and suggestions are also gratefully acknowledged.

REFERENCES

1. V. G. Koppelmann, "Theory of thin film layers of weakly absorbing materials and their application as interferometer mirrors," Ann. Phys. **460**, 388–396 (1960), in German.
2. M. Flannery, E. Loh, and M. Sparks, "Nearly perfect multilayer dielectric reflectors: theory," Appl. Opt. **18**, 1428–1435 (1979).
3. C. Carniglia and J. H. Apfel, "Maximum reflectance of multilayer dielectric mirrors in the presence of slight absorption," J. Opt. Soc. Am. **70**, 523–534 (1980).
4. A. Lakhtakia, "Reflection from a semi-infinite rugate filter," J. Mod. Opt. **58**, 562–565 (2011).

5. Yu. V. Bludov, N. M. R. Peres, and M. I. Vasilevskiy, "Unusual reflection of electromagnetic waves from a stack of graphene layers at oblique incidence," J. Opt. **15**, 114004 (2013).
6. J. Lekner, *Theory of Reflection*, 2nd ed. (Springer, 2016) [The original papers are J. Lekner, "Light in periodically stratified media," J. Opt. Soc. Am. A 11, 2892–2899 (1994) and J. Lekner, "Omnidirectional reflection by multilayer dielectric mirrors," J. Opt. A 2, 349–352 (2000)].
7. J. Lekner, "Reflection by absorbing periodically stratified media," J. Opt. **16**, 035104 (2014).
8. M. Shinn and W. M. Robertson, "Surface plasmon-like sensor based on surface electromagnetic waves in a photonic band-gap material," Sens. Actuat. B **105**, 360–364 (2005).
9. C. Vandenbem, "Electromagnetic surface waves of multilayer stacks: coupling between guided modes and Bloch waves," Opt. Lett. **33**, 2260–2262 (2008).
10. B. Auguié, A. Bruchhausen, and A. Fainstein, "Critical coupling to Tamm plasmons," J. Opt. **17**, 033003 (2015).